

# A three-dimensional heterogeneous DNA sensing surface formed by attaching oligodeoxynucleotide-capped gold nanoparticles onto a gold-coated quartz crystal

Shubo Han, Jianqiao Lin, Munlika Satjapipat, Alfred J. Baca and Feimeng Zhou\*

Department of Chemistry and Biochemistry, California State University, Los Angeles, Los Angeles CA 90032, USA.  
E-mail: fzhou@calstatela.edu

Received (in Cambridge, UK) 9th January 2001, Accepted 21st February 2001  
First published as an Advance Article on the web 13th March 2001

Exposing oligodeoxynucleotide (ODN)-capped Au nanoparticles to a quartz crystal under shear oscillation resulted in the formation of a uniform monolayer containing these nanoparticles or multilayers with islands of the ODN-capped nanoparticles, which, in turn, improved the extent of DNA hybridization.

The development of sensitive and sequence-specific assays of nucleic acids in samples of biological origins has recently been a research area under active pursuit. Thiolated single-stranded oligodeoxynucleotides (HS-ss-ODNs) immobilized onto gold films<sup>1–9</sup> or gold nanoparticles<sup>10</sup> have received a great deal of attention. The use of DNA-capped gold nanoparticles was also shown as an attractive route for enhancing the sensitivities of several important techniques. For instance, a probe/target/probe-nanoparticle sandwich and a dendritic structure based on ODN-capped gold nanoparticles were developed by Zhou *et al.*<sup>11</sup> and by Willner and coworkers,<sup>12</sup> respectively, to amplify the weak quartz crystal microbalance (QCM), or more accurately, the thickness-shear mode sensor (TSM)<sup>5,6</sup> signals inherent in conventional ODN probe/ODN target hybridization based on the use of HS-ss-ODNs. The employment of gold nanoparticles in conjunction with other techniques [e.g. atomic force microscopy (AFM) and surface plasmon resonance spectroscopy<sup>13,14</sup>] were also demonstrated to improve other analytical 'figure of merits', such as selectivity and dynamic range.

We report here a simple procedure for attaching ODN-capped gold nanoparticles onto thin gold films for subsequent hybridization with target DNA molecules. The procedure is devised on the basis of a serendipitous discovery we made in performing a sandwich DNA assay described in ref. 11. We found that ODN-capped gold nanoparticles can be rapidly adsorbed onto a thin, polished gold film that is part of a quartz crystal undergoing shear oscillation (8 MHz fundamental frequency). Curve 1 in Fig. 1 depicts the dramatic frequency decrease resulting from attaching 30-mer-capped gold nanoparticles (*ca.* 890 Hz) upon injecting buffer solutions containing these ODN-capped nanoparticles. The attachment of the ODN-capped gold nanoparticles onto the gold-coated crystal must have arisen from the well known non-specific interaction between the DNA bases and the gold surface,<sup>1,2</sup> since the ODN-capped gold nanoparticles do not possess any affinity for the Au surface with a monolayer coverage of hexanethiol SAM (Curve 2), and the gold nanoparticles alone do not appear to adhere to the gold film (Curve 3). We believe that the shear motion of the thin gold film greatly facilitated a surface rearrangement of the adsorbed ODN-capped gold nanoparticles to form a robust film. The formation of the ODN-capped gold nanoparticle assembly appears to proceed layer-by-layer. AFM images revealed that a compact monolayer of the ODN-capped gold nanoparticle assembly was produced (Fig. 2a) after *ca.* 100 s of exposure of the crystal to an ODN-capped Au nanoparticle solution. The surface morphology of the crystal surface becomes much more uniform as the ODN-capped nanoparticles are within a smaller size distribution than the gold grains originally present at the crystal

(not shown). Thus the surface of crystal was not rougher than the original polished gold film, suggesting that mass changes described below are unlikely to be caused by the effects due to the porosity and/or roughness of the new surface. Extensive exposure of the crystal surface under the shear motion to the solution, on the other hand, leads to the formation of multilayers of ODN-capped gold nanoparticles (Fig. 2b). Individual gold nanoparticles with a size around 13–15 nm can be resolved. Upon exposure for an extended period of time (*e.g.* 8000 s), a purple thin film can actually be visualized. Also notice that, beyond the first layer, it appears that the ODN-capped gold nanoparticles tend to agglomerate preferentially at certain sites to produce islands. These islands, together with the nanoparticle

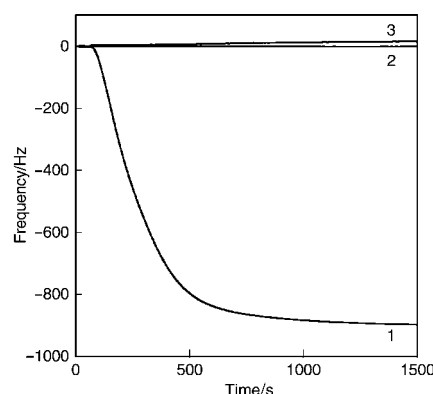


**Fig. 1** QCM responses to the injections of 100  $\mu\text{L}$  solutions containing Au nanoparticles and Au particles capped with HS-ss-DNA of different numbers of DNA bases. Curve 1 shows the response at the crystal surface to the injection of the Au nanoparticles capped with the 30-mer probe with the sequence of 5'-AGAGGATCCCCGGGTACCGAGCTCGAATTC(CH<sub>2</sub>)<sub>6</sub>SH-3'. This sequence is complementary to the 47-mer target 5'-GAATTCGAGCTCGGTACCCGGGGATCCTCTACTGGCCGTCGTTTTAC-3' used in the follow-up hybridization experiment (shown in Fig. 3). Curves 2 and 3 correspond to the responses to a 0.15  $\mu\text{M}$  30-mer-capped Au nanoparticle at a crystal modified with a hexanethiol SAM and to a 0.15  $\mu\text{M}$  Au nanoparticle solution at a crystal, respectively.

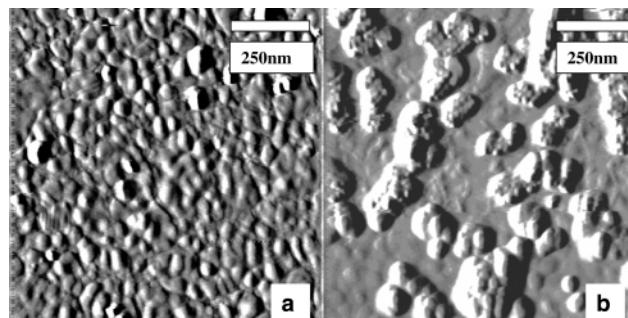


**Fig. 2** AFM images of (a) a gold film covered with the 30-mer-capped gold nanoparticle assembly formed by exposing the gold film to the DNA-capped Au nanoparticle solution for 100 s, and (b) a gold film modified with the 30-mer-capped nanoparticle assembly formed upon an 8000 s exposure.

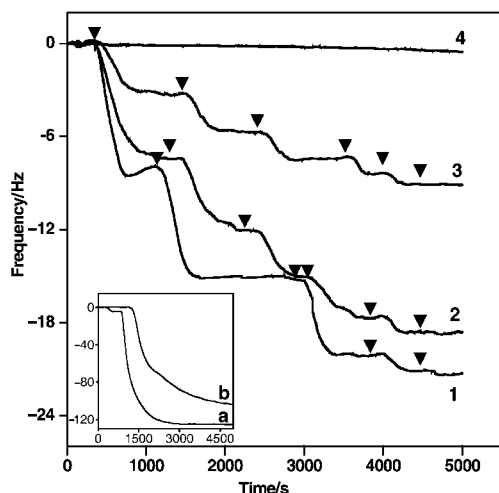


**Fig. 3** QCM responses acquired after the injections of a 47-mer target (5'-GAATTCGAG CTGGTACCCGGGATCCTCTACTGGCCGTCGT-TTAC-3') at a crystal covered with a 30-mer-capped Au nanoparticle assembly (Curve 1), the 47-mer target at a crystal covered with a 16-mer (5'-HS(CH<sub>2</sub>)<sub>6</sub>GTAAAACGACGGCCAG3')-capped Au nanoparticle assembly (Curve 2), the 47-mer target at a crystal covered with a sub-monolayer of 30-mer SAM (Curve 3), and a 47-mer target (5'-CTTGAGAGCTCGG-TACCCGGGATCCTCTACTGGCCGTCGTTTTAC-3') with six of the bases mismatching the bases on the 30-mer probe that had been immobilized onto the gold nanoparticles (Curve 4). Inset: (a) hybridization of the 47-mer target with the 16-mer probe and the frequency change in a subsequent injection of the 30-mer-capped gold nanoparticle solution, and (b) the frequency change upon injecting the 30-mer-capped gold nanoparticle solution into the QCM cell housing a crystal covered with only the 16-mer probe. Arrows indicate the injection points.

terraces that are not covered, thus provide a unique 3-D ODN-capped gold nanoparticle assembly with many sites for DNA hybridization. Fig. 3 shows DNA hybridization at crystals covered with different ODN-capped gold nanoparticles (Curves 1 and 2) and the comparison of the results with those acquired at crystals modified with only HS-ss-ODN (Curve 3). As can be seen, the five consecutive injections of a 3.35  $\mu\text{g mL}^{-1}$  47-mer target solution resulted in a cumulative frequency decrease of *ca.* 22 Hz at a crystal covered with 30-mer-capped gold nanoparticles, whereas the injections of the same target solution at a crystal modified with 16-mer-capped gold nanoparticles produced a 19 Hz change. Both frequency decreases are greater than those observed from multiple injections of the target solution into a QCM housing a 30-mer SAM (*ca.* 9 Hz in Curve 3). Therefore, it seems that more probe molecules are present at the films containing ODN-capped gold nanoparticles since more target molecules can be detected at such films. Previous studies of gold films covered with different ODNs have shown that the surface density of a thiolated 32-mer is slightly less than  $1.8 \times 10^{-11} \text{ mol cm}^{-2}$ .<sup>3</sup> We measured, with an inductively coupled plasma-atomic emission spectrometer, the average gold:sulfur ratio on the 30-mer-capped Au nanoparticles to be 1:87. Using a diameter of 13 nm for the Au nanoparticles,<sup>14</sup> we calculated the surface density to be  $2.7 \times 10^{-11} \text{ mol cm}^{-2}$ . These values correspond to sub-monolayer coverages (*e.g.*  $2.7 \times 10^{-11} \text{ mol cm}^{-2}$  corresponds to *ca.* 49% coverage)<sup>9</sup> and are consistent with those reported in many previous papers.<sup>1,2,4-9</sup> Obviously, the surface density associated with the sub-monolayer of HS-ss-ODN film would not lead to an extensive DNA hybridization at the surface. This contention is in line with the weak QCM signals observed by many research groups<sup>11,15,16</sup> without post-hybridization treatment or target derivatization. Thus, the formation of a multilayer of ODN-capped gold nanoparticles provides a unique means to increase the total number of probes per unit area by converting the ODN assembly at a 2-D surface to a 3-D network. Another implication of the incomplete HS-ss-ODN surface coverage at gold is that the non-specific interaction between ODN and the bare gold regions could lead to an overestimate of the DNA

hybridization when ODN-capped gold nanoparticles were employed to amplify hybridization signals. Indeed, when we performed the sandwich assay using the 16-mer probe on the gold surface and the 30-mer-capped gold nanoparticle as the second probe for signal amplification of the hybridized 47-mer target, most of the frequency decrease appears to result from the non-specific adsorption of the gold nanoparticles onto the gold regions that were not occupied by the 16-mer. As seen in the inset of Fig. 3, Curve a, which shows the frequency change associated with the typical 'sandwich assay',<sup>11</sup> and Curve b, which shows the non-specific adsorption of the 30-mer probes immobilized to the nanoparticles onto the gold surface that has a partial coverage of 16-mer probes, have yielded similar frequency changes. In Curve a, the first step (*ca.* 4.5 Hz) corresponds to the hybridization of the 47-mer target with the 16-mer probe and the second step (*ca.* 126 Hz) is due to the combined effect of non-specific adsorption (*ca.* 108 Hz in Curve b) and the legitimate hybridization of the 30-mer on the gold nanoparticles with the surface-confined 47-mer target.

The comparison between the signal intensities of Curves 1 and 2 indicates that longer ODN probes would cause a larger extent of hybridization. While the longer probes tend to coil more extensively, and consequently impose a greater hindrance to target hybridization, the difference in binding energy between the two different strands should be more predominant for these short ODNs. To ensure that mass changes shown in Curves 1 and 2 in Fig. 3 did not originate from non-specific target adsorption onto the ODN-capped gold nanoparticles films, we conducted a control experiment. The absence of any appreciable frequency change at the 30-mer-capped gold nanoparticle film upon the injections of a target with six mismatched bases confirms that non-specific adsorption did not occur (Curve 4).

In closing, we have developed a method to modify a crystal surface with oligonucleotide-functionalized gold nanoparticles. The attachment of the ODN-capped gold nanoparticles increases the total number of ss-ODN probes available for DNA hybridization. An important point that merits attention is that caution should be exercised when ODN-capped gold nanoparticles are used in connection with the sandwich assay by QCM since non-specific adsorption of the DNA-functionalized gold nanoparticles could lead to an overestimate of the signal enhancement.

## Notes and references

- 1 R. Levicky, T. M. Herne, M. J. Tarlov and S. K. Satija, *J. Am. Chem. Soc.*, 1998, **120**, 9787.
- 2 A. B. Steel, T. M. Herne and M. J. Tarlov, *Anal. Chem.*, 1998, **70**, 4670.
- 3 A. B. Steel, R. L. Levicky, T. M. Herne and M. J. Tarlov, *Biophys. J.*, 2000, **79**, 975.
- 4 D. N. Furlong, F. Caruso, E. Rodda, K. Niikura and Y. Okahata, *Anal. Chem.*, 1997, **69**, 2043.
- 5 B. A. Cavic, G. L. Hayward and M. Thompson, *Analyst*, 1999, **124**, 1405.
- 6 M. Thompson and L. M. Furtado, *Analyst*, 1999, **124**, 1133.
- 7 J. Wang, P. E. Nielsen, M. Jiang, X. Cai, J. R. Fernandes, D. H. Grant, M. Ozsoz, A. Beglieter and M. Mowart, *Anal. Chem.*, 1997, **69**, 5200.
- 8 A. J. Thiel, A. G. Frutos, C. E. Jordan, R. M. Corn and L. M. Smith, *Anal. Chem.*, 1997, **69**, 4948.
- 9 S. O. Kelley, J. K. Barton, N. M. Jackson and M. G. Hill, *Bioconjugate Chem.*, 1997, **8**, 31.
- 10 C. A. Mirkin, *Inorg. Chem.*, 2000, **39**, 2258 and references therein.
- 11 X.-C. Zhou, S. J. O'Shea and S. F. Y. Li, *Chem. Commun.*, 2000, 953.
- 12 F. Patolsky, K. T. Ranji, A. Lichtenstein and I. Willner, *Chem. Commun.*, 2000, 1025.
- 13 L. A. Lyon, M. D. Musick, P. C. Smith, B. D. Reiss, D. J. Pena and M. J. Natan, *Sens. Actuators, B*, 1999, **54**, 118.
- 14 S. Han, J. Lin, F. Zhou and R. L. Vellanoweth, *Biophys. Biochem. Res. Commun.*, 2000, **279**, 265.
- 15 F. Patolsky, A. Lichtenstein and I. Willner, *J. Am. Chem. Soc.*, 2000, **2000**, 418.
- 16 E. Huang, M. Satiapipat, S. Han and F. Zhou, *Langmuir*, 2001, **17**, 1215.